From the standard PID to the CRONE first generation controller: Application to an anti-roll system for Electric Vehicles.

Hussein Termous*/, Xavier Moreau**, Clovis Francis *, Hassan Shraim***

** Lebanese University, Faculty of Engineering, Scientific Research Center in Engineering (CRSI), Campus Rafic Hariri, Beirut, Lebanon, Email: husseintermous@gmail.com; cfrancis@ul.edu.lb; hassan.shraim@gmail.com*

*** University of Bordeaux, Lab IMS CNRS 5218, Talence, Bordeaux, France*
Email: xavier.moreau@ims-bordeaux.fr

Abstract: In this paper, the standard PID controller and the fractional first generation CRONE controller are applied on the anti-roll moment system to improve ride comfort for passengers in the frame of global chassis control of electric vehicles. A comparative study is done showing the performance and the robustness of the two controllers, in frequency and time domain. It is shown that the first generation CRONE control-system is able to provide robust fractional order controller for uncertain perturbed plants.

Keywords: PID, CRONE, fractional order controller, robustness, anti-roll, comfort, global chassis control.

1. INTRODUCTON

Since its introduction, PID controllers have been widely used in industrial control applications (Bennett, 2001). For years, it was the most popular controller, mainly because of its simple parameters and simple structure that need to be used, in addition to the ease with which engineers can implement it using current computer technology (De Oliveira and Karimi, 2012). It has high performance in many control problems, but the performance/robustness analysis of closed-loop systems with PI and PID controllers revealed the existing trade-off between performance and robustness (Garpinger et al., 2014).

In order to achieve more challenging control requirements, the fractional order controllers have received a great attention recently. This kind of controllers are more flexible than the integer-order ones. One approach for fractional order controllers named CRONE, a French acronym of "Commande Robuste d'Ordre Non Entier" which means non-integer order robust controller. The CRONE methodology is a frequency-domain approach for the design of output feedback robust controllers. It is used for continuous-time or discrete-time problems, and for perturbed SISO LTI systems. For the SISO case, three CRONE Control-System Design (CSD) methods have been developed, successively extending the application field (Oustaloup, 1991)(Lanusse, 2010). In this paper, we studied the roll stability enhancement of an electric vehicle by means of two controllers, the standard PID and first generation CRONE controller.

Roll stability is one of the main dynamic factors that needs to be considered in the ground vehicle. It presents a high challenge for vehicle safety. Geometric dimensions, suspension characteristics, and maneuvering conditions influence the dynamic roll behavior of a vehicle. This is also an issue for railroad vehicles with high center of gravity.

To improve the roll dynamics, several vehicles were equipped with active suspension components controlled by different methods of controllers (Chokor et al., 2016), like the Hydractive, CRONE (Moreau et al., n.d.) (Moreau et al., 2009), and BOSE (Brown, 2005). One example of active suspension system is the one introduced in the Active Wheel (Laurent et al., 2000) (Fig.1).

Fig. 1. Active wheel from Michelin.

This kind of active wheels is mostly used in light electrical cars, where two in-wheel 30-kW motors motorize it. The suspension system is composed of a spring and an electric engine. This system offers new perspectives in the suspension control, which indeed offers important opportunities in global chassis control. It can provide safer steering using the active roll control system by compensating roll dynamics when manoeuvring. The principle of the controller is to provide an anti-roll moment opposes the one results from vehicle manoeuvring.

Depending on the design methodologies introduced in (Abi Zeid Daou et al., 2013; Morand et al., 2016), the PID and the first generation CRONE controllers are designed to control the roll dynamics of the vehicle's chassis. The synthesis model is implemented for an anti-roll system that is embedded in the electric vehicle, and the main objective of this control process is to reduce the body roll dynamics for ride comfort and decreasing rollover propensity. The effectiveness of both controllers will be studied in the frame of their performance and robustness against uncertain parameters. The results obtained in the frequency and time domains are compared, revealing the advantages and drawbacks of each controller.

After this introduction, section 2 gives the context. Section 3 introduces the synthesis model. Section 4 shows the robustness and performance analysis. Finally, a conclusion and the prospects.

2. CONTEXT

A high-level controller named "The supervisor" is responsible for computing the needed anti-roll moment. This moment is then transferred to every suspension actuator embedded in the Active Wheels as reference forces to provide the needed moment around the roll axis. Fig. 2 shows the complete Global Chassis Control diagram, where the supervisor takes as an input all the measured signals needed, and provides as an output the reference for the different actuators (steering, traction, braking, and local active suspensions). The objective of the supervisor is to estimate first the life situation of the vehicle based on a set of available measurements.

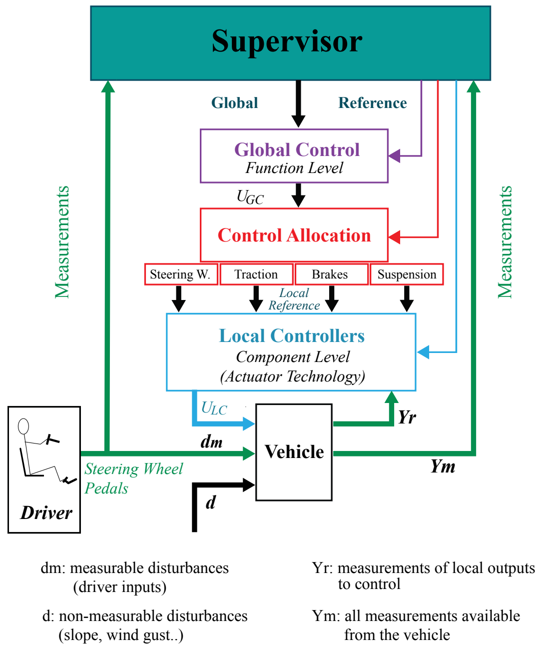

Fig. 2. Global Chassis Control diagram.

As shown in Fig.3, according to the estimated value or the measured values of the lateral acceleration a_y and the longitudinal acceleration a_x of the vehicle, the supervisor can estimate the life situation of the vehicle. Then the supervisor selects the best control strategy associated with the detected field of operation of the vehicle, and finally generates the reference signals for all actuators.

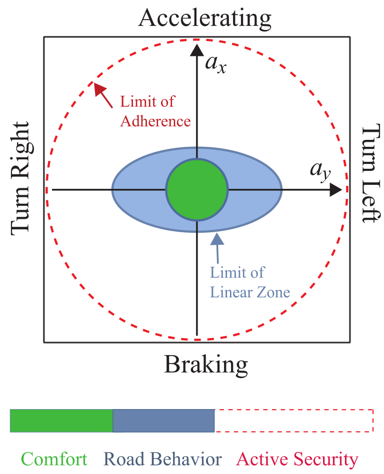

Fig. 3. Vehicle situations.

The controller variables associated with the centre of gravity of the vehicle are: The longitudinal velocity $V_x(t) = V_{x_{ref}}(t)$, the yaw rate $\dot{\psi}(t) = \dot{\psi}_{ref}(t)$, and the main three dynamics of the chassis: the velocity of vertical displacement $\dot{z}_G(t)$, the pitch rate $\dot{\varphi}_G(t)$, and the roll rate $\dot{\theta}_G(t)$ such that:

$$\dot{z}_G(t) = 0, \quad \dot{\varphi}_G(t) = 0, \quad \text{and} \quad \dot{\theta}_G(t) = 0. \tag{1}$$

In this study we are focusing in one the above goals, which is $\dot{\theta}_G(t) = 0$. This should achieve a good compensation of roll dynamics around the roll axis that consequently will improve ride comfort. Assuming that the vehicle is operating in the green region (Fig. 3), then the longitudinal velocity is considered constant ($V_x(t) = cst,\ a_x(t) = 0$), and a stable maneuvering, with a fixed radius R, leads to a constant value of lateral acceleration estimated by:

$$a_y(t) = \frac{V_x^2(t)}{R} = cst < 0.4g. \tag{2}$$

2.1. Synthesis Model

Consider the following equation that represents the roll dynamics (Newton's second law):

$$\omega_G(t) = \dot{\theta}_G(t) = \frac{1}{I_{xx}} \int_0^t c_{\Sigma x}(\tau) d\tau + \dot{\theta}_G(0), \tag{3}$$

where I_{xx} is the inertia moment of the sprung mass with respect to the roll axis, and $c_{\Sigma x}(\tau)$ is the algebraic sum of the exterior torques applied on the roll axis of the vehicle. It consists of two terms:

$$c_{\Sigma x}(t) = c_{r0}(t) + c_{ar}(t). \tag{4}$$

$c_{r0}(t)$ is the roll couple introduced to the system as a perturbation and is equal to the following:

$$c_{r0}(t) = H\ M_T\ a_y(t), \tag{5}$$

where H is the height of the center of gravity of the vehicle, and M_T is the total mass of the vehicle. The term

$c_{ar}(t)$ is the anti-roll torque provided by the anti-roll system. It results from the summation of two inputs:

- The feedback control input:

$$C_{FB}(s) = -K_{ar}(s)\Omega_G(s). \tag{6}$$

- The feedforward command input:

$$c_{FF}(t) = -H_{nom}\, M_{Tnom}\ \lambda\, \tilde{\theta}_v(t). \tag{7}$$

Knowing that $K_{ar}(s)$ is the controller, $\Omega_G(s)$ is the output roll rate, g is the gravity, $H_{nom} = 0.55\, m$ is the nominal height of the chassis, $M_{Tnom} = 600\, kg$ is the nominal total mass of the vehicle, $\lambda = 6.11\, ms^{-2} rad^{-1}$, and $\tilde{\theta}_v(t)$ is the measured steering angle. The controlled plant, as formulated in (3) with zero initial conditions, is $P(s) = 1/(I_{xx}s)$ as in Fig.4, where $N(s)$ represents the noise measurements. For passive system, the anti-roll torque $c_{ar}(t)$ is given by:

$$c_{ar}(t) = b_\theta \omega_G(t) + k_\theta \int_0^t \omega_G(\tau) d\tau + c_{ar}(0), \tag{8}$$

where b_θ is the coefficient of viscous friction at the centre of gravity resulting from the four dampers of the vehicle in [Nm s/rad], and k_θ is the stiffness coefficient resulting from the four springs and 4 anti-roll bars in [Nm/rad]. Then the passive suspension can be presented as shown in Fig. 5, by a transfer function $K(s)$ similar to one of the PI regulator as the following equation with $C_p = b_\theta$ and $\omega_{1p} = k_\theta / b_\theta$:

$$K(s) = C_{PI}(s) = b_\theta + \frac{k_\theta}{s} = C_p\left(\frac{1 + s/\omega_{1p}}{s/\omega_{1p}}\right). \tag{9}$$

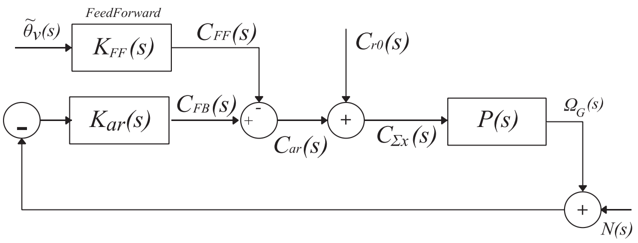

Fig. 4. Anti-roll system diagram.

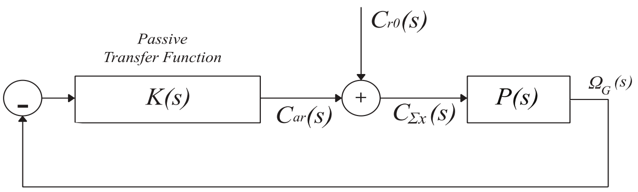

Fig. 5. Passive anti-roll system diagram.

Fig. 6 shows the Bode responses for the three plants showing the gain variation results from the variation of I_{xx} shown in Table 1, where the phase angles are constant.

Table 1. Variation of Uncertain parameters.

	min	med	max
$M_T\ [kg]$	600	750	900
$I_{xx}\ [kg.m^2]$	150	225	300

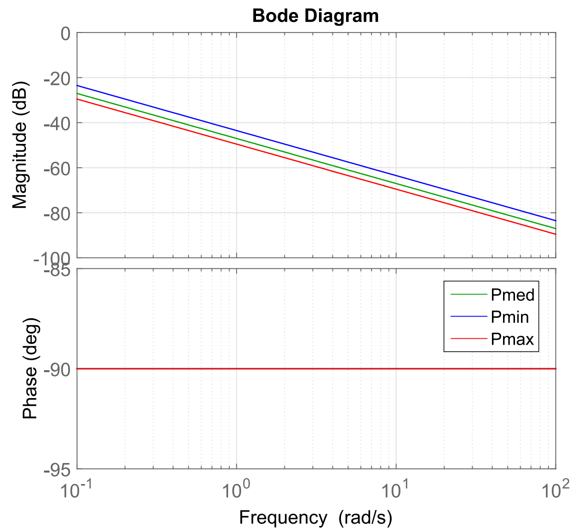

Fig. 6. Bode diagrams of uncertain models.

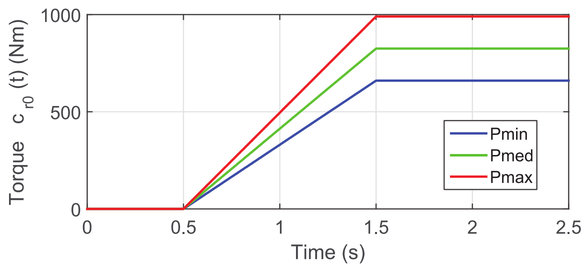

Fig. 7. Introduced perturbations into the three plants.

2.2. Signal Modelling

In order to achieve our objective, the reference value of roll rate chosen to be zero ($\omega_{Gref} = 0$). The perturbations $c_{r0}(t)$ (rolling couple) introduced to the systems have a ramp profile, results from a left manoeuvring for a given steering angle as shown in Fig. 7.

2.3. User Constraints (nominal case)

Different user constraints need to be specified in order to design the two controllers. For this application, the constraints are given as:

- The crossover frequency $\omega_u = 2\pi 10\ rad/s$, which is about four times rapid than that of the frequency of the driver. Knowing that the range of driver frequency is [0 – 2.5] Hz.
- The phase margin $M_\phi > M_{\phi min} = 40°$.
- Zero static error.
- Torque control limit : $max\ [c_{ar}(t)] < 16\,000\ N$.

3. CONTROLLERS

To obtain a significant comparison between PID and first generation CRONE controllers, two requirements should be respected: Iso-rapidity, which means same crossover frequency ω_u of the open loop system. Second, the Isodegree of stability, which means same M_ϕ. In this paper, phase margin is given as $M_\phi = 45°$. For both controllers $Pnom = Pmin$, where $Pnom$ is the nominal plant.

3.1. PID Controller

According to (Abi Zeid Daou et al., 2013; Morand et al., 2016) and for $\omega_m = \omega_u$ and $\phi_1 = 60°$, the transfer function of PID controller obtained is as follows:

$$C_{PID}(s) = 3616\left(\frac{1+s/108.8}{s/108.8}\right)\left(\frac{1+s/48.2}{1+s/82}\right). \quad (10)$$

3.2. First Generation CRONE Controller

As ordered in (Abi Zeid Daou et al., 2013; Morand et al., 2016), and choosing $\omega_B = \omega_u$, $A = B = 10$, and $m_l = m_h = 1$, the computed fractional first generation transfer function is as follows:

$$C_{frac}(s) = 37607\left(\frac{1+s/3.94}{s/3.9}\right)\left(\frac{1+s/3.94}{1+s/628}\right)^{0.5}\left(\frac{1}{1+s/628}\right). \quad (11)$$

Then, the parameters and the recursive zeros and poles of the rational transfer function are shown in Table 2.

Table 2. Parameters of CRONE controller.

Parameter	Value (rad/s)	Parameter	Value (rad/s)
N	4	ω_{z3}	68.5
$\alpha\,\eta$	3.55	ω_{z4}	243
α	1.884	ω_{p1}	10.2
η	1.884	ω_{p2}	36.3
ω_{z1}	5.4	ω_{p3}	129
ω_{z2}	19.3	ω_{p4}	458

Finally, the rational transfer function $C_{rat}(s)$ can be represented as:

$$C_{rat}(s) = 37607\left(\frac{1+s/3.94}{s/3.94}\right)\prod_{i}^{N=4}\frac{1+s/\omega_{zi}}{1+s/\omega_{pi}}\left(\frac{1}{1+s/628}\right). \quad (12)$$

Fig.8 shows the bode diagrams of both controllers where it can be seen that they present the same gain and phase at ω_u.

4. PERFORMANCE ANALYSIS

In this section, the robustness analysis is presented for both controllers with the feedback control input only (without the feedforward part), in the frequency and time domain. Then the performance analysis is presented for the controlled anti-roll systems, including the feedforward control part, applied on 14 DOF model (Morand et al., 2016)

4.1. Robustness analysis in frequency domain

Fig. 9 shows the Bode plot responses of the open loop transfer functions for both controllers. Fig. 10 represents the Nichols loci obtained with two controllers. It is shown that for nominal case, both have same rapidity (ω_u) and same degree of stability ($M\phi$).With CRONE controller (Fig. 10-b), the phase margin remains constant for a range of frequencies where ω_u can vary. This illustrates the stability degree robustness versus gain uncertainties in frequency domain. Fig. 11 and 12 present the different sensitivity functions obtained with PID and CRONE controller. It is obvious that with CRONE, $T(s)$ and $S(s)$ have a robust factor of resonance.

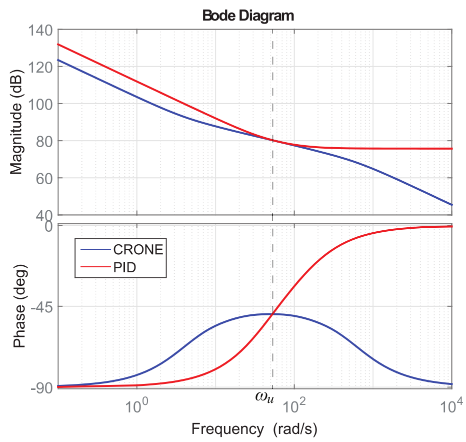

Fig. 8. Bode diagram representing the two controllers in frequency domain.

4.2. Robustness analysis in time domain

Fig. 13 shows the command input $c_{ar}(t)$ of each controller while introducing a disturbance having a step profile of magnitude $c_{r0} = 500N$ to the closed loop system. It is shown in Fig.13-b, with CRONE controller, that the three models have the same first overshoot and that the damping remains constant. This illustrates the stability degree robustness versus gain uncertainties in time domain.

4.3. Performance of the Anti-Roll System with 14 DOF Model

In the following, a comparison done between the performance of the passive anti-roll system, an anti-roll system with PID controller, and an anti-roll system with first generation CRONE controller. Fig. 14, 15 and 16 show the effectiveness of the controlled systems over the passive system in compensating roll dynamics, the roll rate, the roll angle and roll acceleration respectively. In addition to that, Table 3 presents the numerical results obtained comparing the results of controlled systems with respect to the passive one. It is clear that both controllers achieved a satisfied performance, with very high compensation, in which the human body cannot perceive them. Moreover, the command signals produced by the controllers are also presented in Fig. 17, in comparison with the perturbation introduced.

4. CONCLUSION

This article presents the effectiveness of the first generation CRONE control in achieving robustness in time and frequency domain, in spite of variation of the plant parameters. The two controllers show their good performance in compensating the roll dynamics, which improve ride comfort for passengers. The next step of this work is to implement these controllers with the other local controllers in the frame of Global Chassis Control.

Table 3. Time domain numerical results.

	Roll motion (max[controller]/max[Passive])		
	Acceleration	Rate	Angle
PID	0.1035	0.0327	0.0271
CRONE	0.1242	0.0579	0.0706

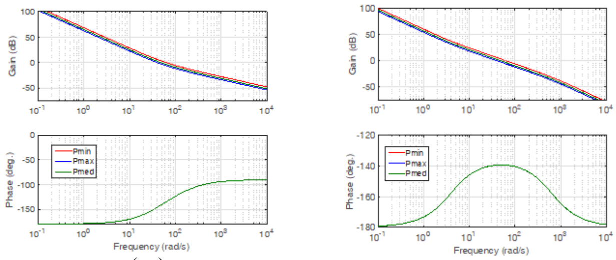

(a) (b)

Fig. 9. Open loop bode diagram: (a) PID, (b) CRONE

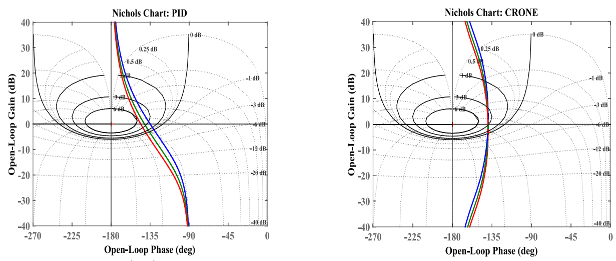

(a) (b)

Fig. 10. Open-loop Nichols plot with: (a) PID, (b) CRONE.

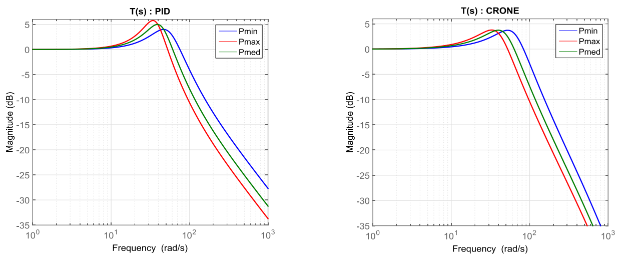

(a) (b)

Fig. 11. *T(s)* obtained with: (a) PID, (b) CRONE.

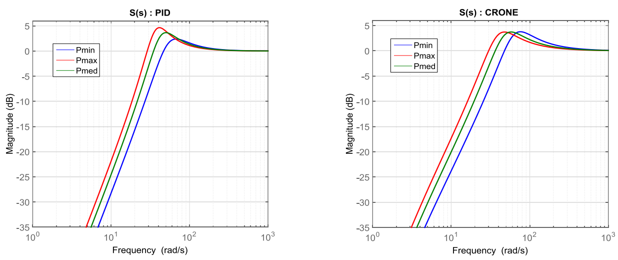

(a) (b)

Fig. 12. *S(s)* obtained with: (a) PID, (b) CRONE.

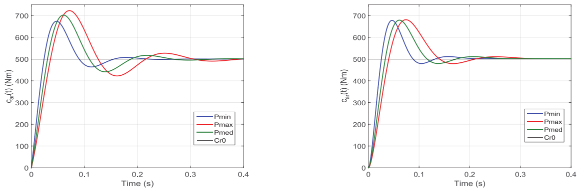

(a) (b)

Fig. 13. Step responses obtained with: (a) PID, (b) CRONE.

ACKNOWLEDGEMENT

This work was supported by the Lebanese research program and the AUF-CNRSL-UL program.

REFEFRENCE

Abi Zeid Daou, R., Moreau, X., Francis, C., 2013. Regulation of a pump-tank-sensor system using two fractional-order controllers. J. Appl. Nonlinear Dyn. 2, 355–371.

Bennett, S., 2001. The past of PID controllers. Annu. Rev. Control 25, 43–53. https://doi.org/10.1016/S1367-5788(01)00005-0

Brown, S.N., 2005. Vehicle suspension.

Chokor, A., Talj, R., Charara, A., Shraim, H., Francis, C., 2016. Active suspension control to improve passengers comfort and vehicle's stability, in: 2016 IEEE 19th International Conference on Intelligent Transportation Systems (ITSC). pp. 296–301. https://doi.org/10.1109/ITSC.2016.7795570

De Oliveira, V., Karimi, A., 2012. Robust and gain-scheduled PID controller design for condensing boilers by linear programming. IFAC Proc. Vol. 2, 335–340. https://doi.org/10.3182/20120328-3-IT-3014.00057

Garpinger, O., Hägglund, T., Åström, K.J., 2014. Performance and robustness trade-offs in PID control. J. Process Control 24, 568–577. https://doi.org/10.1016/j.jprocont.2014.02.020

Lanusse, P., 2010. CRONE control system design, a CRONE toolbox for Matlab.

Laurent, D., Sebe, M., Walser, D., 2000. Assembly comprising a wheel and a suspension integrated into the wheel.

Morand, A., Moreau, X., Melchior, P., Moze, M., Guillemard, F., 2016. CRONE cruise control system. IEEE Trans. Veh. Technol. 65, 15–28. https://doi.org/10.1109/TVT.2015.2392074

Moreau, X., Oustaloup, A., Nouillant, C., n.d. From analysis to synthesis of vehicle suspensions : the CRONE approach. Eur. Control Conf. ECC'99.

Moreau, X., Rizzo, A., Oustaloup, A., 2009. Application of the CRONE control-design method to a low-frequency active suspension system. Int. J. Veh. Auton. Syst. 7, 172–200.

Oustaloup, A., 1991. La commande CRONE. Hermès, Paris.

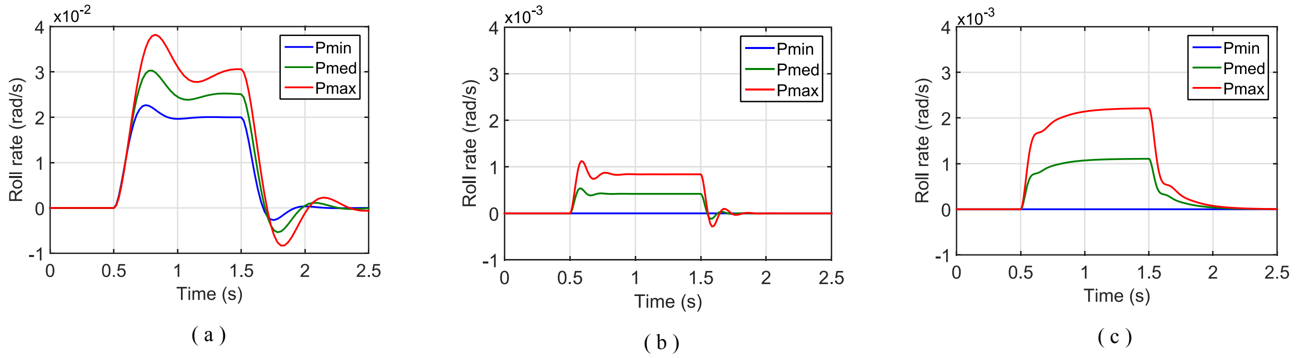

Fig. 14. Roll rate (a) Passive, (b) PID , and (c) CRONE.

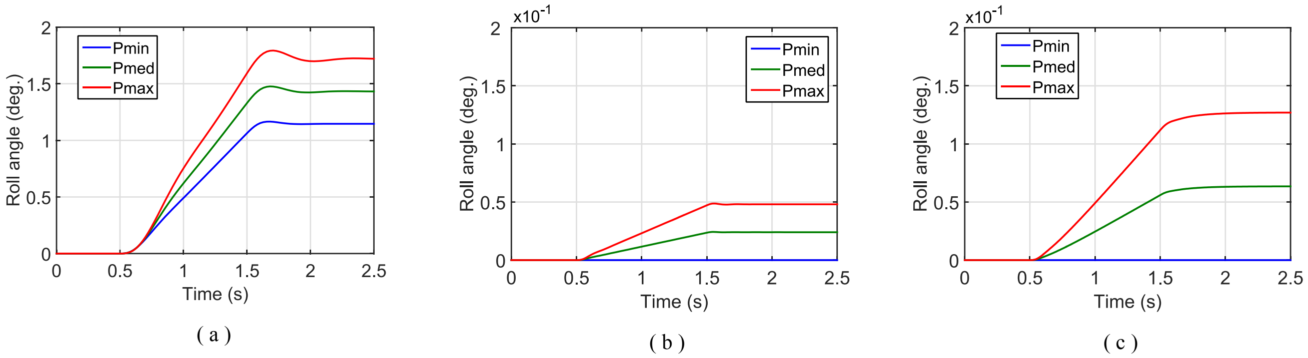

Fig. 15. Roll angle (a) Passive, (b) PID , and (c) CRONE.

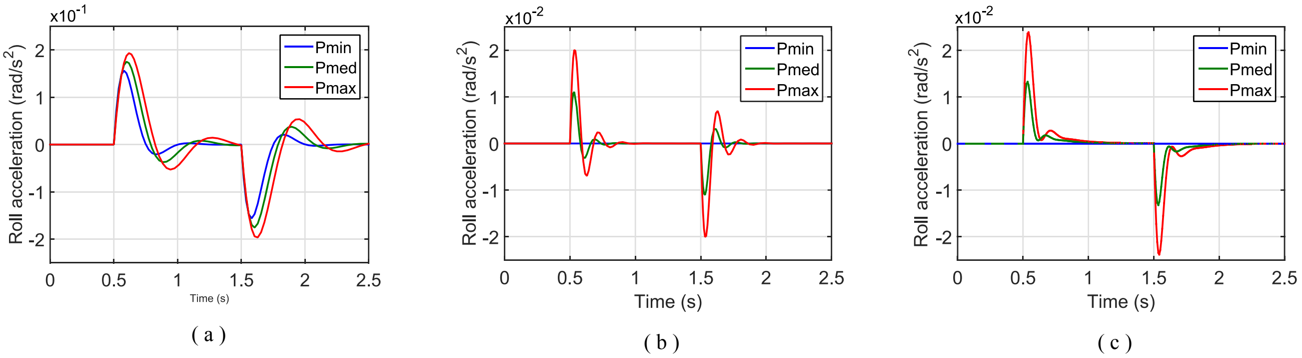

Fig. 16. Roll acceleration: (a) Passive, (b) PID , and (c) CRONE.

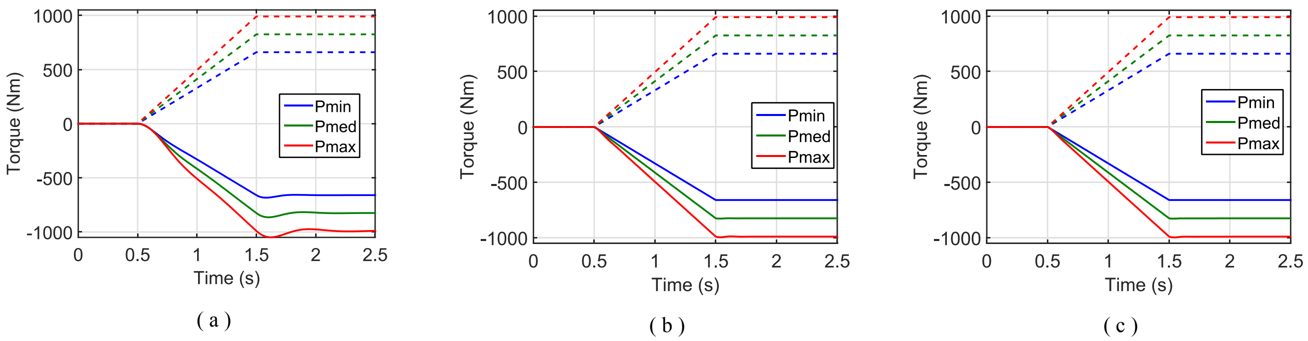

Fig. 17. Torques $c_{r0}(t)$ '– –' and $c_{ar}(t)$ '—' : (a) Passive, (b) PID , and (c) CRONE.